Flux-line lattices in artificially layered superconductors

A. M. Thompson and M. A. Moore
Theory Group, Department of Physics, University of Manchester, Manchester M13 9PL, United Kingdom
(Received 25 August 1997)

The flux-line lattice of superconductors has been investigated when there exists a periodicity in the underlying system, such as can occur in artificially layered structures. For small fields parallel to the layers the flux lines enter the sample in sequential rows, with the possibility of jumps in the magnetization as new rows are created. As the field is increased these discontinuities gradually decrease, but there still exist transitions between states that are aligned differently to the periodic direction. Increasing the magnitude of the periodic potential reduces the competition between differently aligned lattices and tends to lock in one particular alignment. The effect of transitions on the shear modulus is also discussed and related to the experiments of Theunissen *et al.* [Phys. Rev. Lett. **77**, 159 (1996)]. [S0163-1829(98)03921-6]

I. INTRODUCTION

The nature of the flux-line lattice in superconductors still attracts much interest. For an isotropic system the equilibrium lattice is known to be triangular. We will investigate situations where this may not be the case. In particular we shall impose a one-dimensional periodic structure on an infinite superconductor, and use this periodicity to model an underlying potential. This allows us to model, for example, some of the behavior of artificially layered structures when the field is applied parallel to the layers.

The interplay between the flux-line lattice and an underlying periodic potential has already been investigated for many different superconducting systems. These include thin films with modulated thickness,[1] Pb-Bi alloys with periodic concentration of Bi,[2] Pb/Ge multilayers with a lattice of submicron holes,[3] superconducting wires with an hexagonal array of artificial pins,[4] and spatially modulated Josephson junctions.[5]

Using London theory, Brongersma *et al.*[6] modeled the magnetization of thin Nb-Cu multilayers with the applied field almost parallel to the layers. The magnetic induction was allowed to change by permitting the size of the system to vary while keeping the number of flux lines fixed. As the applied field was increased, a series of maxima in the magnetization was observed. This was due to the flux lines reorganizing within the sample, where transitions occurred between states where the flux lines form rows that divide the sample into equal parts. This situation has also been investigated by numerically solving the time-dependent Ginzburg Landau equations coupled to Maxwell's equations in a homogeneous isotropic superconducting thin film.[7] As the field applied parallel to the film was increased the magnetization also showed a series of maxima. Away from these maxima there was a series of discontinuities in the magnetization as more flux lines penetrated into the sample.

Critical currents also show similar behavior. Discontinuities in the critical current have been observed at specific matching fields where the numbers of rows change. The positions of the maxima in the critical currents is sensitive to the system used, with YBa_2CuO_7 (YBCO), $Bi_2Sr_2CaCu_2O_8$ (BSCCO), and NbCu multilayers showing different field dependences.[8,9,10]

We investigate here the properties of flux lines within an infinite system, under the influence of a potential with period L_y in the $\hat{\mathbf{y}}$ direction. We take the applied field to be in the $\hat{\mathbf{z}}$ direction. This infinite system contains a principal region of width L_y and approximates a layered system. In the absence of the potential, it is well known that flux lines form a periodic lattice with hexagonal symmetry in an infinite system. With the periodic potential the flux lines may form a lattice that is commensurate with the principal region and we investigate rectangular and centered rectangular structures with this property. The rectangular structure has basis vectors in the $\hat{\mathbf{x}}$ and $\hat{\mathbf{y}}$ planes, and the centered rectangular structure, shown in Fig. 1, is characterized by the angle 2ϕ between the basis vectors. For two different ϕ the centered rectangular lattice will be the triangular lattice expected in a pure infinite system. These correspond to $\phi=\pi/6$ and $\phi=\pi/3$. Figures 1(a) and 1(b) show $\phi=\pi/6$ and $\phi=\pi/3$, respectively. The state with $\phi=\pi/6$ has the base of its equilateral triangle aligned perpendicular to the periodic direction. Conversely, in the state with $\phi=\pi/3$ the base is aligned parallel to the periodic direction. We distinguish between these two states by referring to the centered rectangular structure with $\phi=\pi/6$ as the lattice aligned parallel to the periodic direction (the $\hat{\mathbf{y}}$ axis) and the structure with $\phi=\pi/3$ as the lattice aligned perpendicular to the periodic direction.

On minimizing the Gibbs free energy it is found that the equilibrium lattice usually has ϕ only approximately $\pi/6$ or $\pi/3$, but the above distinction regarding alignments is used. The equilibrium lattice is often a competition between these two alignments, and this competition is most readily seen when the periodic potential is very weak.

As the applied field is varied two distinct types of transitions are observed between some of these different structures. The simplest, type A, transitions just involve the number of rows of flux lines within the principal region increasing by one, with no realignment of the lattice. Type B transitions occur between states aligned differently to the periodic direction, and during these transitions the number of rows changes significantly.

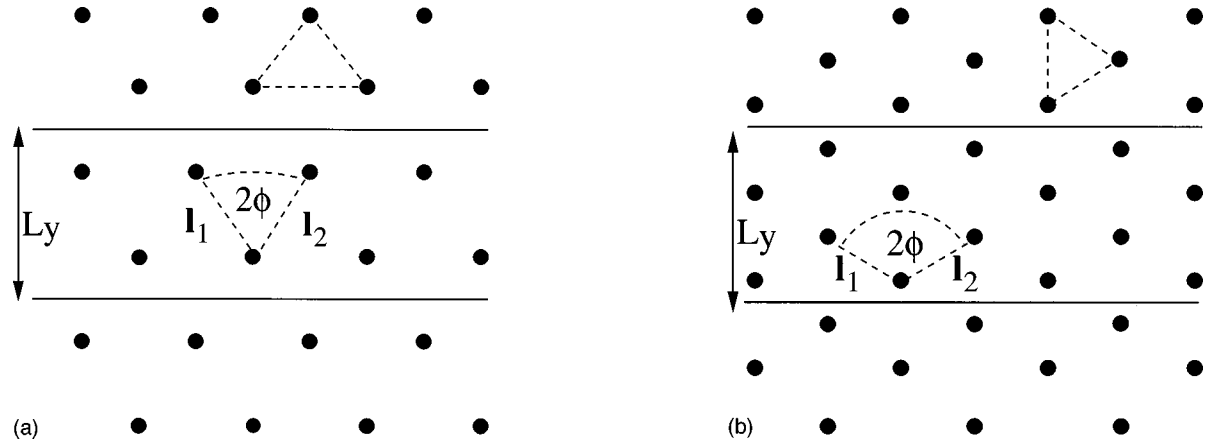

FIG. 1. A multilayered superconducting structure, with the field applied parallel to the layers. The solid circles represent the flux lines, which form a lattice commensurate with the principal region, a strip of width L_y. The lattices shown are centered rectangular structures, whose basis vectors are separated by the angle 2ϕ. The figure shows (a) $\phi=\pi/6$ and (b) $\phi=\pi/3$.

The periodic potential can be chosen to favor having the flux lines close to either the edges or the center of the principal region. This ensures that one of the alignments of the flux-line lattice is favored over the other. The sequence of transitions therefore can be changed by increasing the strength of the underlying potential.

The model used to investigate the flux-line lattice is developed in Sec. II. The formalism discussed concentrates on the lowest-Landau-level (LLL) limit in the mean field approximation. Throughout we shall neglect thermal fluctuations. The transitions are also investigated in the London limit. For many of these transitions notable jumps in the magnetization are observed. This is not the only property that can be affected by the periodicity of the system. Some of the consequences of the periodicity are developed in Sec. IV, where we investigate in particular the shear modulus c_{66}. It ''oscillates'' in a manner similar to that seen in experiments by Theunissen *et al.*[9]

Theunissen *et al.*[9] investigated the properties of a NbN/Nb_3Ge bilayer under the influence of an applied current and magnetic field. A regular array of channels was etched through the thin NbN top layer into the Nb_3Ge. The NbN layer, with its much higher critical current than the Nb_3Ge layer, effectively acted as a pinning center for the flux lattice. By measuring the shearing force needed for the flux lines to move along the channels, the shear modulus of the flux-line lattice could be measured. The shear modulus shows a characteristic behavior $c_{66}\propto b(1-b)^2$ as the field is increased. In the London limit $c_{66}\propto b$, while in the LLL limit $c_{66}\propto(1-b)^2$. Superimposed on this functional form was an oscillatory function that reflected the finite nature of the channel width. While the geometry of our calculations does not match that in their experiment precisely, it becomes a better approximation to it as the width of the Nb_3Ge channels is increased relative to the width of the unetched NbN rows. In this situation the pinning effect of the NbN rows can be modeled by a periodic potential which encourages the location of vortices at the channel edges.

II. BASIC FORMALISM

The experiments of Theunissen *et al.*[9] suggest the possibility of transitions between different configurations of flux lines both in the limit of low magnetic induction where London theory will be valid, namely, where $c_{66}\propto b$, and at higher inductions where $c_{66}\propto(1-b)^2$ when the LLL is more appropriate. We investigate the LLL first.

The Ginzburg-Landau free energy is

$$\mathcal{F}[\Psi]=\int d^3r\left[\alpha(T)|\Psi(r)|^2+\frac{\beta}{2}|\Psi(r)|^4-\frac{1}{2m}\Psi(r)^*D^2\Psi(r)+\frac{1}{2\mu_0}B^2\right], \tag{1}$$

where $D^2=\mathbf{D}\cdot\mathbf{D}$, $\mathbf{D}=-i\hbar\nabla-2e\mathbf{A}$, and the magnetic induction $\mathbf{B}=\nabla\times\mathbf{A}$. The LLL assumes the magnetic screening length is infinite. We will use the Landau gauge where $\mathbf{A}=Bx\hat{\mathbf{y}}$, and ignore fluctuations in the magnetic field. In the LLL the order parameter is expanded in the set of eigenfunctions of D^2, using only the degenerate states which have the lowest eigenvalue. In the rectangular geometry these degenerate states are

$$\Psi_p=\exp\left(-ipk_0y-\frac{1}{2l_m^2}(x-pk_0l_m^2)^2\right), \tag{2}$$

where l_m is the magnetic length $l_m=(\Phi_0/2\pi B)^{1/2}$ and k_0 is the wave vector in the y direction whose value is determined by the boundary conditions. The general LLL order parameter is of the form $\Psi=Q\Sigma_{p=-\infty}^{\infty}c_p\Psi_p$, which is periodic in the y direction over a length $L_y=2\pi/k_0$. Obviously states which do not have this high degree of periodicity of their order parameter at the mean field level could exist for a layered system. We shall ignore them as even with the imposed periodicity the phase diagram at the mean field level is extremely rich. [9]

In an infinite system, the equilibrium configuration of flux lines is known to be that of a triangle.[11] In our problem the flux lines are imagined to interact weakly with an underlying periodic potential due to the layering. Although we ignore the direct contributions of it to the energy at this point, we assume that this potential acts to impose the periodicity L_y on the ordered state. Hence, the flux lines form a lattice that is commensurate with the principal region and repeats over a distance l_y, which must be a simple fraction of L_y, i.e., l_y

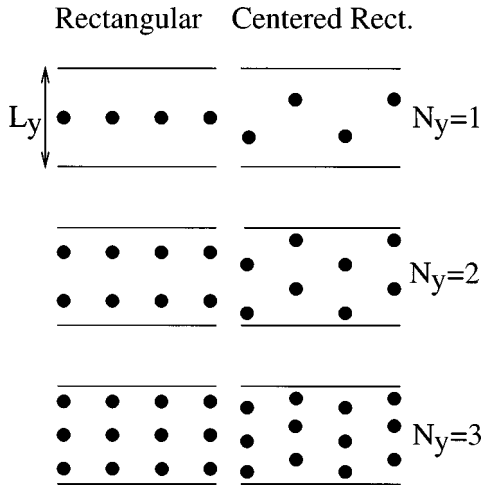

FIG. 2. The flux-line lattices with rectangular and centered rectangular symmetry. These lattices are commensurate with the principal region, which is a strip of width L_y. The equilibrium lattice is predominantly a centered rectangular lattice.

$=L_y/N_y$, where N_y is an integer equal to the number of rows of flux lines in the principal region. We investigate rectangular and centered rectangular structures with this property as shown in Fig. 2. The flux line lattice with rectangular symmetry has basis vectors $\mathbf{l}_1=l_y\hat{\mathbf{y}}$ and $\mathbf{l}_2=l_x\hat{\mathbf{x}}$. The centered rectangular structure, also shown in Fig. 1, has basis vectors $\mathbf{l}_1=-l_x\hat{\mathbf{x}}+l_y\hat{\mathbf{y}}/2$ and $\mathbf{l}_2=l_x\hat{\mathbf{x}}+l_y\hat{\mathbf{y}}/2$, and is characterized by the angle 2ϕ between these two vectors. The model used is shown for a centered rectangular structure, but is easily modified for the rectangular lattice.

Within the LLL the mean field line H_{c_2} is defined by $\alpha_B=0$ where $B=H_{c_2}$ and $\alpha_B=\alpha(T)+eB\hbar/m$. Using the linearized expression for $\alpha(T)$, $\alpha(T)=-\alpha'(1-t)$ then $\alpha_B=-\alpha'(1-t-b)$ where t is the reduced temperature T/T_{c0} and b is the reduced field B/B_{c0}. T_{c0} is the mean field transition temperature while B_{c0} is the straight line extrapolation of H_{c_2} to zero temperature. The temperature is conveniently represented by the dimensionless parameter $\alpha_T=\alpha_B(\pi\hbar L_z/\beta eBk_BT)^{1/2}$, where L_z is the sample thickness along the field direction. Low temperatures are represented by $\alpha_T\rightarrow-\infty$ while high temperatures correspond to $\alpha_T\rightarrow+\infty$. The rescaled free energy per flux line is then

$$\mathcal{F}_{flux}=-\frac{k_BT\alpha_T^2}{2\beta_A(R)}+\frac{B^2}{2\mu_0}A_{flux}L_z, \tag{3}$$

where $A_{flux}=\Phi_0/B$ is the area per flux line. The ratio $R=l_y/2l_x$, as used by Kleiner *et al.*,[11] characterizes the lattice. Figure 3 shows the dependence of the Abrikosov parameter β_A on the ratio R, and it should be noted that $\beta_A(R)=\beta_A(1/R)$, where $\beta_A=\langle|\Psi|^4\rangle/(\langle|\Psi|^2\rangle^2)$. The square lattice corresponds to $R=1$ and the minima in $\beta_A(R)$ occur for the equilateral triangular lattice, with $R=1/\sqrt{3}$ and $R=\sqrt{3}$. These two minima correspond to the two alignments of the flux lattice relative to the periodic direction. The state with $\phi=\pi/6$ in Fig. 2(a) corresponds to the minima at $R=\sqrt{3}$ and the state with $\phi=\pi/3$ has $R=1/\sqrt{3}$.

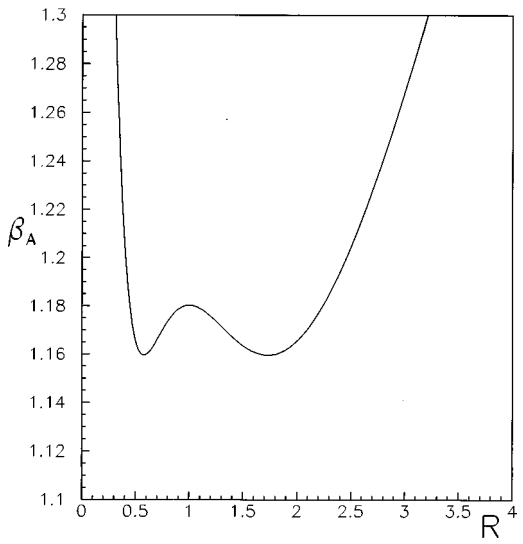

FIG. 3. The dependence of β_A on the ratio $R=l_y/2l_x$. It should be noted that $\beta_A(R)=\beta_A(1/R)$.

For a given field B, the free energy per unit volume, F_{vol}, depends solely on the parameter R. If we minimize F_{vol}, the flux line lattice will be arranged in the configuration that minimizes $\beta_A(R)$, while keeping $B=2RN_y^2(\Phi_0/L_y^2)$. For small fields $B<\Phi_0/L_y^2$ the equilibrium configuration corresponds to $N_y=1$ as the smallest value of $\beta_A(R)$ corresponds to $N_y=1$. As the field is increased there will be transitions between configurations of different N_y and equal β_A. The transition between states $N_y=1$ and $N_y=2$ occurs when $B=4\Phi_0/L_y^2$.

For larger fields the transitions occur between states near the minima of β_A. Most transitions occur between states with $R\approx1/\sqrt{3}$ but there are a few transitions to and from states near the minimum at $R=\sqrt{3}$. All these transitions occur for constant B between states of equal $\beta_A(R)$ with a change in N_y.

III. GIBBS FREE ENERGY

To understand the possibilities of transitions between different states at constant H the relevant quantity to minimize is not the free energy per flux line, but rather the Gibbs free energy per unit volume $\mathcal{G}_{vol}$. The Gibbs free energy per flux line can be written as

$$\mathcal{G}_{flux}=-\frac{\alpha_T^2k_BT}{2\beta_A}+\frac{1}{2\mu_0}(B-\mu_0H)^2L_ZA_{flux}. \tag{4}$$

Rewriting this in terms of the reduced fields the Gibbs free energy per flux line becomes

$$\mathcal{G}_{flux}=\frac{1}{2}\alpha_T^2k_BT\left\{2\kappa^2\left(\frac{b-h}{1-t-b}\right)^2-\frac{1}{\beta_A}\right\}, \tag{5}$$

where $h=\mu_0H/B_{c0}$. Although α_T is the single intensive parameter that characterizes the free energy $\mathcal{F}$, it is necessary to show the explicit dependence on the average induction B. Therefore, since $\mathcal{G}_{vol}=\mathcal{G}_{flux}B/\Phi_0L_Z$, at constant H and T,

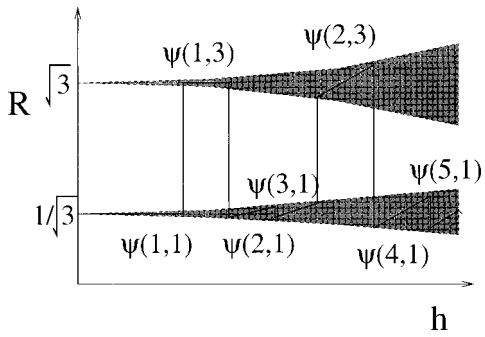

FIG. 4. A representation of how R changes as h increases. The range of values of R that minimize the Gibbs free energy is shown within the shaded region.

$$\mathcal{G}_{vol}(H,T,B)=\frac{1}{2}\mu_0 H_c^2 g(h,t,b),$$

$$g(h,t,b)=2\kappa^2(b-h)^2-(1-t-b)^2/\beta_A, \qquad (6)$$

where b is the reduced magnetic field $b=2RN_y^2(2\pi\xi^2/L_y^2)$ and ξ is the coherence length defined through the upper critical field $H_{c_2}=\sqrt{2}\kappa H_c=\Phi_0/2\pi\xi^2$. The behavior of the system is therefore controlled by κ and $b_0=2\pi\xi^2/L_y^2$.

If the applied field h is small, the Gibbs energy $g(h,t,b)$ is dominated by the term $(1-t-b)^2/\beta_A$. The minimum free energy flux line configuration is obtained by being as close as possible to having $R=1/\sqrt{3}$ or $R=\sqrt{3}$. The range of allowed values of b is small, and as h is increased there is a series of first order transitions at which the lattice reconstructs. As the lattice undergoes a reconstruction between different states $\Psi(N_y,\sqrt{3}R)$ there are jumps in the magnetic induction b. Except for the transition $\Psi(1,1)\rightarrow\Psi(1,3)$ this involves a change in the number of ''rows'' of flux lines and these reconstructions can be classified into two categories. The simplest involve just an increase in the number of rows for two states with $R\approx 1/\sqrt{3}$ or $R\approx\sqrt{3}$. Some of these type A transitions include $\Psi(2,1)\rightarrow\Psi(3,1)$ and $\Psi(4,1)\rightarrow\Psi(5,1)$ and occur between states with the same alignment to the periodic direction. The other set of transitions involves a change in the alignment of the flux-line lattice. The type B transitions occur between states near the different minima of $\beta_A(R)$ and involve either a *reduction* in the number of rows combined with a large increase in R or an *increase* in the number of rows and a reduction in R. These transitions include $\Psi(3,1)\rightarrow\Psi(2,3)$ and $\Psi(4,3)\rightarrow\Psi(7,1)$. By putting in ascending order the values of KN_y^2 where $K=1/\sqrt{3}$ or $\sqrt{3}$ we can see the appropriate sequence of states. This sequence of states looks similar to that in the previous section, but the states possess a smaller range of values of R. Transitions occur between states with different β_A, different b, and different N_y (see Fig. 4).

For very large applied fields, such that $2\kappa^2(b-h)^2$ is the dominant term in $g(h,t,b)$, there is a wide range of equilibrium values of R that are obtained as h is varied. The lattice distorts from a triangular lattice to ensure $b\approx h$. However, transitions between states with different N_y still occur, but these transitions involve very small changes in the magnetic induction b. As the applied field h is increased there is a smooth crossover between these two limits as the two terms in $g(h,t,b)$ compete with each other. This results in the allowed values of R spreading out from the two values of $1/\sqrt{3}$ and $\sqrt{3}$.

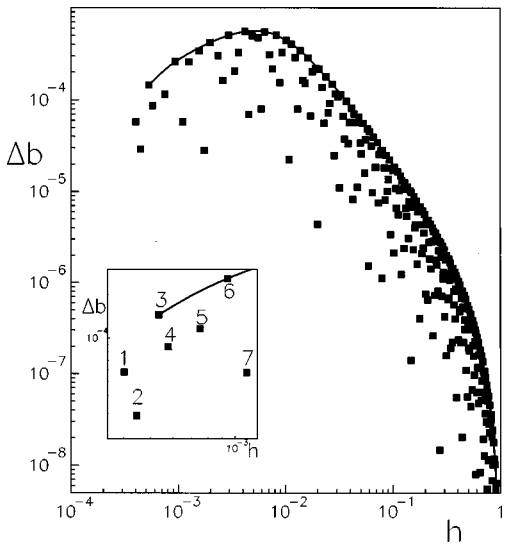

FIG. 5. The jumps in the magnetization vary as the applied field is increased, decaying to zero in the limit $h\rightarrow 1$; for $L_y=10\lambda$, $\kappa=50$. The points indicate the change in the magnetization when the potential is very weak. The heavy line is a guide to the eye, whose physical significance is discussed in the next section.

These transitions can be found by looking at the allowed values of R that minimize the Gibbs free energy. The transitions corresponding to small fields h are between states defined by R being very close to either $1/\sqrt{3}$ or $\sqrt{3}$. As h increases, the range of values of R that minimize the free energy increases, and this leads to the fractional jump in b dropping.

The size of the jumps in the magnetic induction associated with these transitions is given in Fig. 5. These jumps increase at small h as approximately $h^{1/2}$ but decay to zero in the limit $h\rightarrow 1$ following the heavy curve in Fig. 5. The inset describes in detail the initial transitions, showing the points lying on or below the start of the heavy line. Within the LLL approximation the flux lines are not excluded from the sample at small h as $H_{c_1}=0$. The flux lines always form a centered rectangular structure and we only consider behavior for magnetic inductions larger than B_{min}. This is the magnetic induction that corresponds to a simple triangular lattice with $N_y=1$ and $R=1/\sqrt{3}$. The first point in the inset corresponds to the transition between states $\Psi(1,1)$ and $\Psi(1,3)$. The subsequent sequence of these centered rectangular structures is $\Psi(2,1)$, $\Psi(3,1)$, $\Psi(2,3)$, $\Psi(4,1)$, $\Psi(5,1)$ and is easily predicted to the limit $h\rightarrow 1$. The type A transitions, such as $\Psi(2,1)\rightarrow\Psi(3,1)$ (point 3) and $\Psi(4,1)\rightarrow\Psi(5,1)$ (point 6), lie very close to the heavy line. All the other points in the inset describe type B transitions, $\Psi(1,1)\rightarrow\Psi(1,3)$ (point 1), $\Psi(1,3)\rightarrow\Psi(2,1)$ (point 2), $\Psi(3,1)\rightarrow\Psi(2,3)$ (point 4), $\Psi(2,3)\rightarrow\Psi(4,1)$ (point 5), and $\Psi(5,1)\rightarrow\Psi(3,3)$ (point 7). The type B transitions tend to lie well below the heavy line, and these transitions involve a large change in the number of rows. The heavy line describes the situation when type A transitions only occur, which can happen when the strength of the potential is increased. This is discussed in Sec. V.

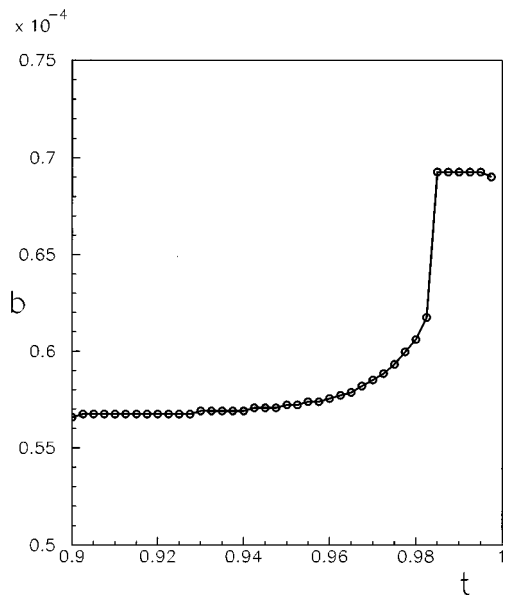

FIG. 6. The ''melting'' transition between states with $N_y=8$ and $N_y=9$ for $h=6.9\times10^{-4}$, $B_0=2\times10^{-6}$.

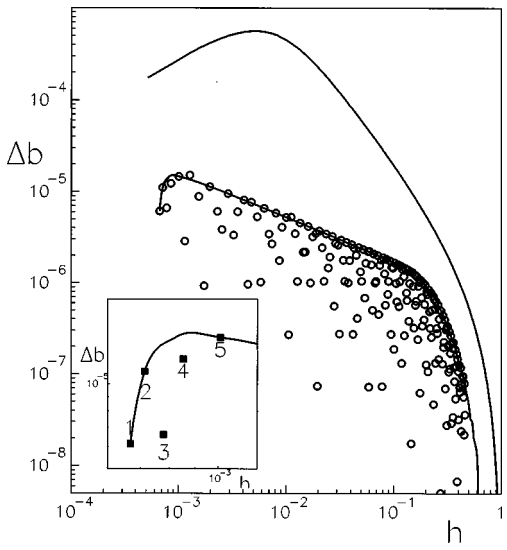

FIG. 7. The change in the magnetization as a function of the applied field h for $L_y=10\lambda$ and $\kappa=50$. The upper heavy line shows the jumps associated with the LLL.

The transitions can also be observed as the temperature is varied. For small N_y these ''melting'' transitions only occur over a very small range of the applied field h. As the range of allowed values of R increases the range of field over which the lattice can be seen to melt also increases. Figure 6 shows the transition between states $\Psi(8,\geqslant1)$ and $\Psi(9,\leqslant1)$.

The LLL will not be strictly applicable in the limit of small b. The LLL approximation may be valid only in the region where $\partial\Delta b/\partial h<0$ in Fig. 5. By increasing b_0 it is possible to shift the maximum in $\Delta b(h)$ to smaller values of N_y but the London theory should be used to investigated the properties of the system with small values of N_y.

IV. LONDON THEORY

The London free energy is

$$\mathcal{F}_{Lon}=\frac{1}{2\mu_0}\sum_{ij}\int\int d\mathbf{r}_i^{\alpha}V_{\alpha\beta}(\mathbf{r}_i-\mathbf{r}_j)\,d\mathbf{r}_j^{\beta}, \qquad (7)$$

where $V_{\alpha\beta}(\mathbf{r})$ is the potential defining the local magnetic induction $B(\mathbf{r})^{\beta}=\Sigma_i\int d\mathbf{r}_i^{\alpha}V_{\alpha\beta}(\mathbf{r}-\mathbf{r}_i)$, the parameters $\{\alpha,\beta\}$ correspond to the $\{x,y,z\}$ components, and $\{i,j\}$ sum over the contributions from all flux lines. We investigate an isotropic system, where the Fourier transform of the London potential for straight flux lines is $\tilde{V}_{\alpha\beta}(\mathbf{k})=\delta_{\alpha\beta}S(\mathbf{k})/(1+\lambda^2k^2)$, λ being the London penetration depth. The cutoff function $S(\mathbf{k})=\exp(-\xi^2k^2)$ removes the divergences within London theory due to the absence of the flux line cores. The use of different cutoffs within London theory has been discussed previously.[12]

We use similar geometries to the previous section and minimize $\mathcal{G}_{Lon}=\mathcal{F}_{Lon}-B\cdot H$ with respect to the positions of the flux lines. Again we assume the flux lines form a lattice commensurate with the principal region.

The low-field behavior using the LLL was dominated by the minimum in $\beta_A(R)$. It might be thought that using London theory could remove the multiplicity of transitions.

The equilibrium lattice is always a centered rectangular structure, and the flux lines do not initially enter the principal region in a single straight row. This is different from a thin slab geometry, where straight rows of flux lines (rectangular symmetry) are frequently the equilibrium structure due to the surface barrier.[6,13]

The flux lines enter as a centered rectangular structure with $N_y=1$, and there is a smooth crossover from $\Psi(1,<1)$ to $\Psi(1,>3)$. The first transition occurs between states $\Psi(1,>3)$ and $\Psi(2,<1)$, and the sequence of structures observed is then the same as the LLL limit. At each of the transitions there is an associated jump in the magnetic induction, but Fig. 7 shows that these are smaller than in the LLL limit. Again, during the type B transitions [point 3, $\Psi(3,1)\rightarrow\Psi(2,3)$, and point 4, $\Psi(2,3)\rightarrow\Psi(3,1)$] the change in the magnetization is much smaller than during the type A transitions [point 2, $\Psi(2,1)\rightarrow\Psi(3,1)$, and point 5, $\Psi(4,1)\rightarrow\Psi(5,1)$] nearby. Therefore, despite the absence of the pronounced minimum in the Gibbs free energy the flux-line lattice shows similar behavior to the LLL limit and the same sequence of states is observed.

V. NONZERO POTENTIAL

In the previous section, the potential has not only been assumed to be periodic, i.e., $V(y)=V(y+L_y)$, but also to only restrict the choice of suitable flux-line lattices. This may be either an extremely weak potential or one whose contribution to the total energy is zero. Now we investigate the equilibrium lattice when the periodic potential does contribute to the overall energy. We define the potential only in the principal region $V(y)=V_0[\cosh(ay)-1]$ where $-L_y/2<y<L_y/2$ and assume the potential is periodic as described above. The potential is zero in the center of the principal region, but depending on the sign of V_0 will either attract or repel flux lines form the edges of the principal region. This

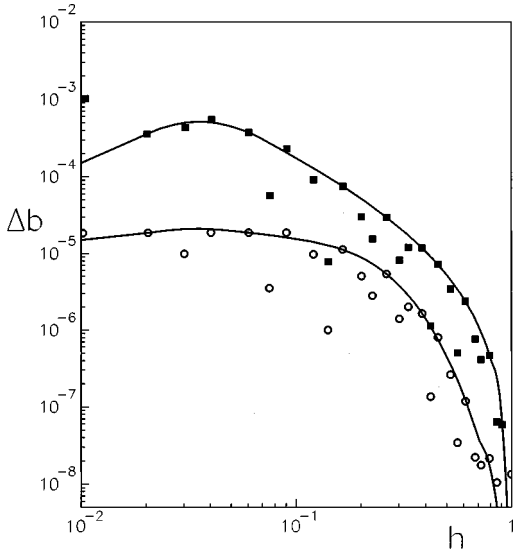

FIG. 8. The changes in the magnetization for $L_y=\lambda$, showing both the LLL limit (solid squares) and the London limit (open circles).

potential then favors states with $R=1/\sqrt{3}$ or those with $R=\sqrt{3}$. Assuming that the potential is still weak, we include just the first order correction $\langle\Psi|V(y)|\Psi\rangle$ to the ground state energy.

The potential favors the type A transitions between states near the same minimum of $\beta_A(R)$ and the inclusion of this potential reduces the number of type B transitions. As V_0 is increased it is then possible to remove transitions between the two minima in $\beta_A(R)$ and for transitions to occur between states with $R\sim 1/\sqrt{3}$ or between states with $R\sim\sqrt{3}$. In a figure analogous to Fig. 4 the allowed values of R would be one shaded band or the other and there would be no transitions between them.

The repulsive (attractive) potential ensures that the lattice chooses alignments aligned parallel (perpendicular) to the periodic direction, i.e., the $\hat{\mathbf{y}}$ direction. The jumps in the magnetic induction follow the heavy curve in Fig. 5. This behavior also occurs in the London limit, where the inclusion of a potential again favors the existence of states permanently aligned either parallel or perpendicular to the y axis.

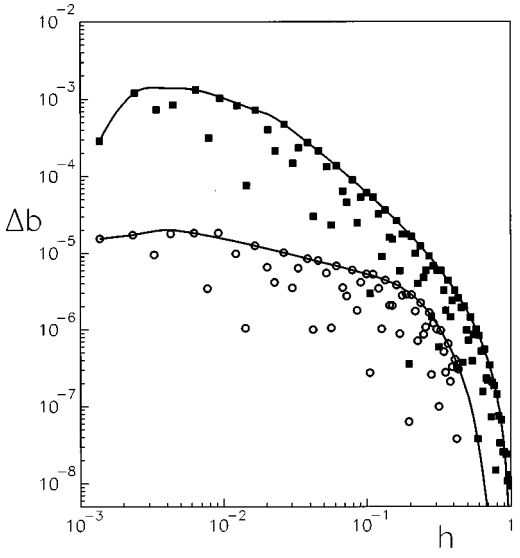

FIG. 9. The changes in the magnetization for $L_y=\sqrt{10}\lambda$ showing both the LLL limit (solid squares) and the London limit (open circles).

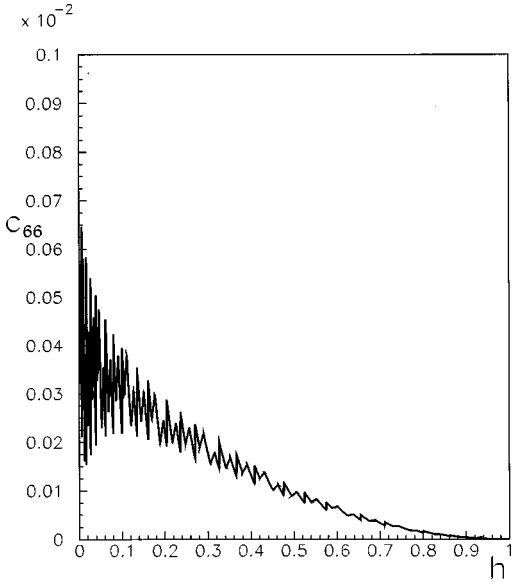

FIG. 10. The shear modulus for the commensurate flux line lattice with no added potential, showing the oscillatory nature as a function of the magnetic induction, for $L_y=\sqrt{10}\lambda$ and $\kappa=50$.

The behavior in Fig. 5 for $L_y/\lambda=10$ is controlled by B_0. Reducing the width of the periodic potential at fixed penetration depth λ, the maximum in $\Delta b(h)$ moves slightly, to smaller N_y. Figures 8 and 9 show the jumps in the magnetization for different widths. The LLL (solid squares) and the London limit (open circles) are shown together and can be compared with Figs. 5 and 7. The heavy lines indicate the transitions that occur in the strong potential limit, and all transitions disappear in the limit $h\rightarrow 1$. The behavior is very similar for the three different widths shown, but increasing the width increases the number of transitions observed.

The shear modulus $c_{66}\propto\partial^2 F_{vol}/\partial\alpha^2$ where α is the shear angle. In the LLL limit, $F_{vol}\propto 1/\beta_A$. The Abrikosov parameter can be written as a sum over all reciprocal lattice vectors $\mathbf{Q}$, $\beta_A=\Sigma_{\mathbf{Q}}\exp -Q^2/2U^2$, where U is the inverse magnetic length $U^2=2\pi/A_{unit}$, A_{unit} being the area of the unit cell. This allows direct calculation of the shear modulus for all lattices.

The modulus changes dramatically as the lattice reconstructs. Figure 10 shows c_{66} in the LLL, where the oscillations characterize the rearrangement of the flux-line lattice within the channel. This shows more oscillations than the experiments of Theunissen *et al.*,[9] but the introduction of the (attractive) potential models the experiments more closely. This would seem natural if one regards the NbN regions in their experiment as regions where the potential has a tendency to trap vortices since an attractive potential encourages vortices to be more at the edges of the channel. The size and positions of the transitions that Theunissen *et al.*[9] observed indicate transitions only with $\Delta N_y=+1$ and for $R\sim\sqrt{3}$. Therefore, the effects of the interaction of the flux lines with the underlying periodic potential are likely to be important,

although the interaction with impurities may hinder extensive reconstructions with large changes in N_y.

VI. CONCLUSION

For an infinite system it is well known the flux lines form a periodic lattice with hexagonal symmetry. Once there is competition with an underlying potential this is not necessarily the situation. The flux lines still favor lattices close to this ideal lattice, and transitions can be seen between different structures. Using both London theory and the LLL approximation we have investigated some of the properties associated with these structures. As the applied field is increased there are notable jumps in the magnetic induction and, hence, in the magnetization and critical current. These transitions occur in two ways. Type A transitions just involve an increase in the number of rows of flux lines in the principal region. Type B transitions occur between states aligned parallel and perpendicular to the periodic direction. The different alignments of the lattice correspond to the two competing minima in $\beta_A(R)$. Increasing the strength of the periodic potential ensures that one of these alignments is favored over the other and eventually only type A transitions increasing the number of rows occur. For V_0 less (greater) than zero, the potential favors the flux lines being at the edges (center) and the flux-line lattice is aligned parallel (perpendicular) to the periodic direction.

The transitions are most easily seen as the applied field is increased. However, they also occur as the temperature is varied and the lattice can appear to melt as the temperature is increased. Also associated with these transitions are changes in the physical properties of the flux-line lattice, such as the shear modulus. The matching fields and the nature of the c_{66} indicate that the experiments of Theunissen *et al.*[9] are best modeled by an attractive potential, which pulls the flux lines to the edges of the region.

ACKNOWLEDGMENTS

It is a pleasure to thank S. Bending for stimulating conversations. This work was supported by EPSRC through Grant No. GR/J60681.

[1] P. Martinolli, M. Nsabimana, G. A. Racine, and H. Beck, Helv. Phys. Acta **55**, 655 (1982).
[2] H. Raffy, E. Guyon, and J. C. Renard, Solid State Commun. **14**, 431 (1974).
[3] V. V. Metlushko, M. Baert, R. Jonckeere, V. V. Moshchalkov, and Y. Bruynseraede, Solid State Commun. **91**, 331 (1994).
[4] L. D. Cooley, P. J. Lee, and D. C. Larbalestier, Appl. Phys. Lett. **64**, 1298 (1994).
[5] V. A. Oboznov and A. V. Ustinov, Phys. Lett. A **139**, 481 (1989).
[6] S. H. Brongersma, E. Verweij, N. J. Koeman, D. G. de Groot, and R. Griessen, Phys. Rev. Lett. **71**, 2319 (1993).
[7] C. Bolech, G. C. Buscaglia, and A. Lopez, Phys. Rev. B **52**, 15 719 (1995).
[8] M. Ziese, P. Esquinazi, P. Wagner, H. Adrian, S. H. Brongersma, and R. Griessen, Phys. Rev. B **53**, 8658 (1996).
[9] M. H. Theunissen, E. Van der Drift, and P. H. Kes, Phys. Rev. Lett. **77**, 159 (1996).
[10] O. Brunner, J. M. Triscone, L. Antognazza, L. Meiville, M. G. Karkut, and O. Fischer, J. Less-Common Met. **164**, 1186 (1990).
[11] W. H. Kleiner, L. M. Roth, and S. H. Autler, Phys. Rev. **133**, A1226 (1964).
[12] A. M. Thompson and M. A. Moore, Phys. Rev. B **55**, 3856 (1997).
[13] G. Carneiro, Phys. Rev. B **57**, 6077 (1998).